

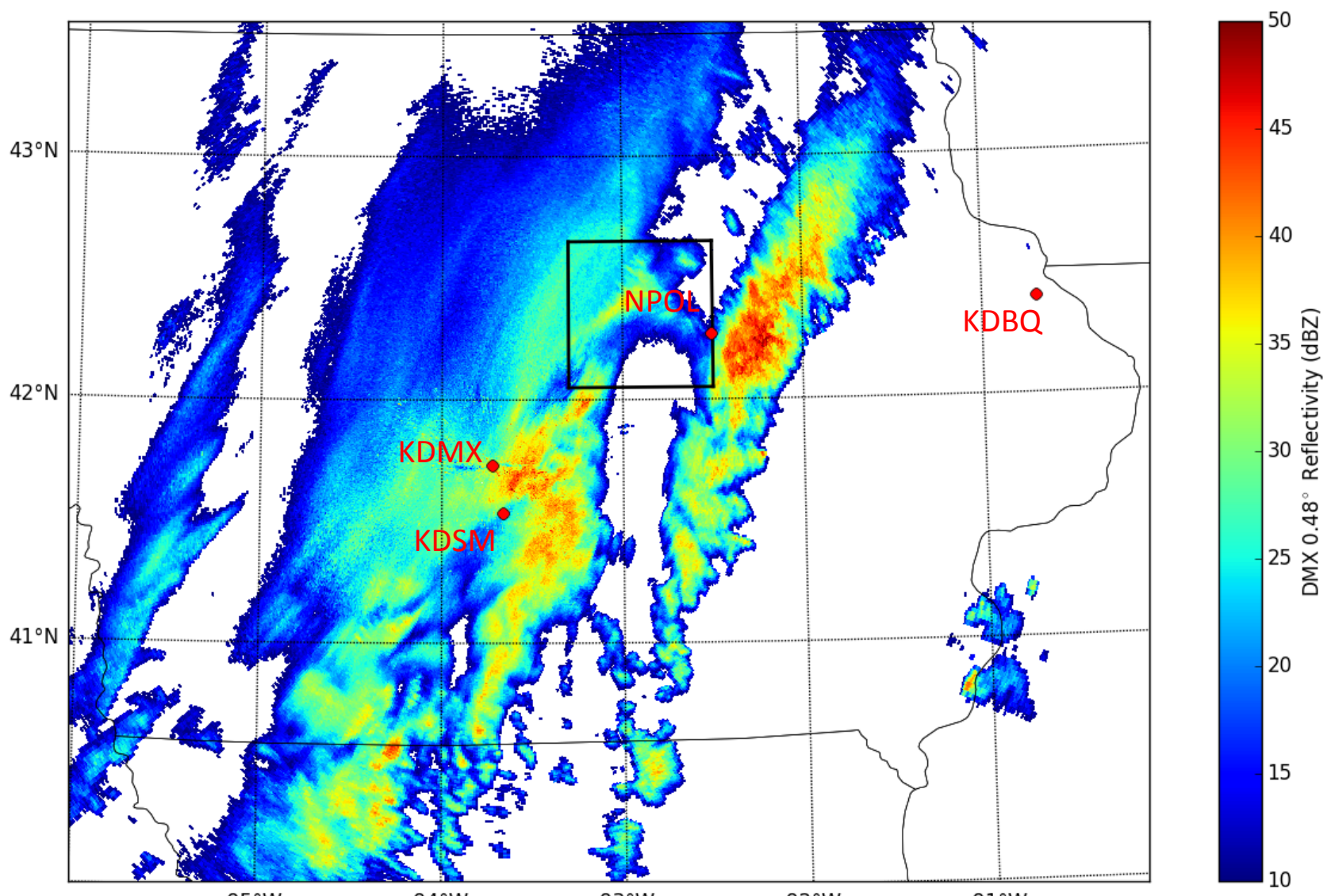


241: NPOL Observations of Kelvin-Helmholtz Waves during the May 2013 IFloodS Campaign

Joseph P. Zagrodnik, Lynn McMurdie, Robert A. Houze, Jr., University of Washington



Introduction/Site Locations



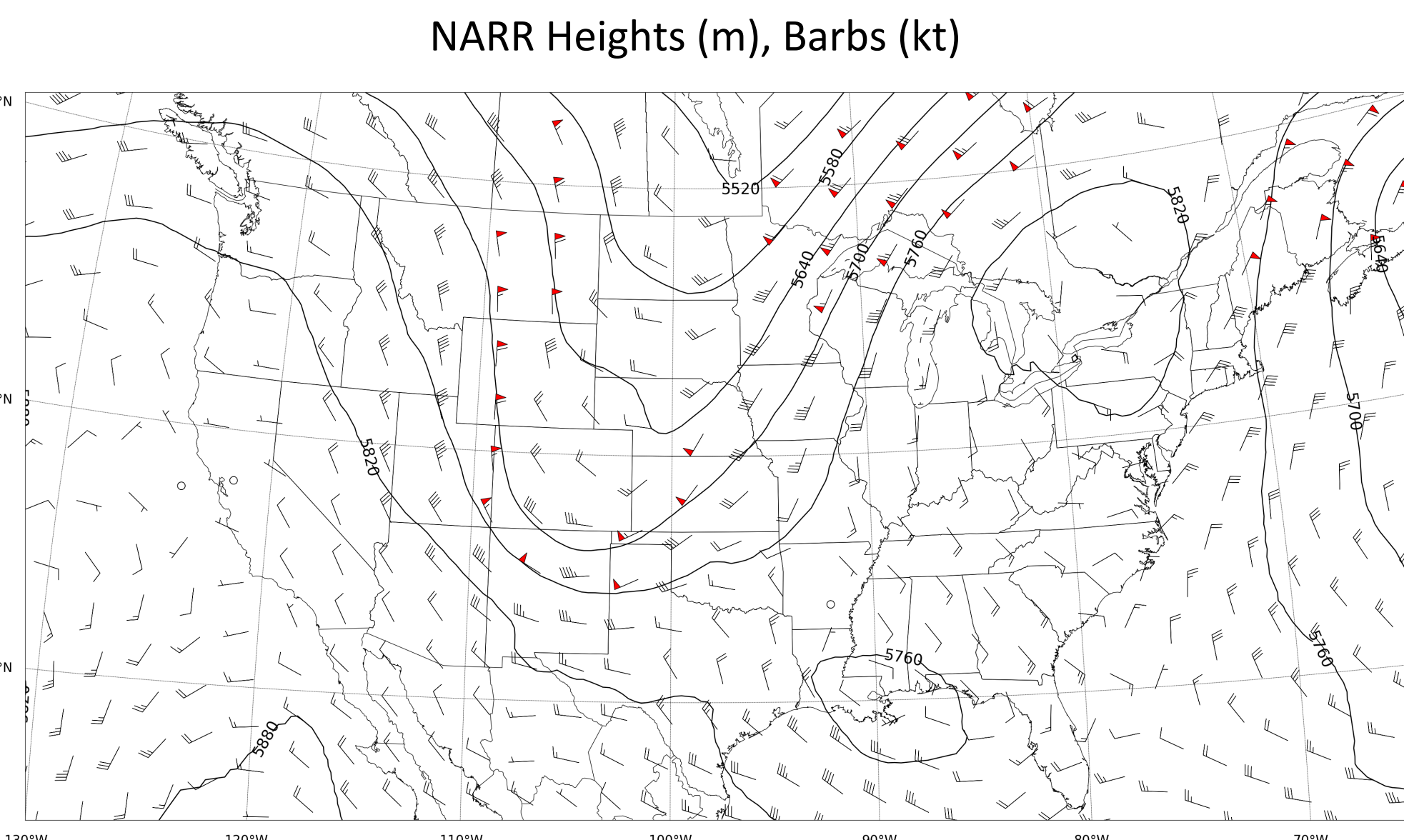
Large-scale KDMX 0.48° radar reflectivity depicting the frontal band of precipitation over Iowa at the time of the wave observations (May-02 12:53 UTC). The waves occurred within the black box.

This poster demonstrates that these are Kelvin-Helmholtz (KH) waves. They share several features in common with the KH-waves observed in Chapman and Browning (1997) and Houser and Bluestein (2011), including formation mechanisms, evolution, and enhancement of precipitation microphysics.

An unprecedented late-season winter storm brought record-breaking snowfall to Iowa during the first week of the IFloodS field campaign, May 02-05, 2013.

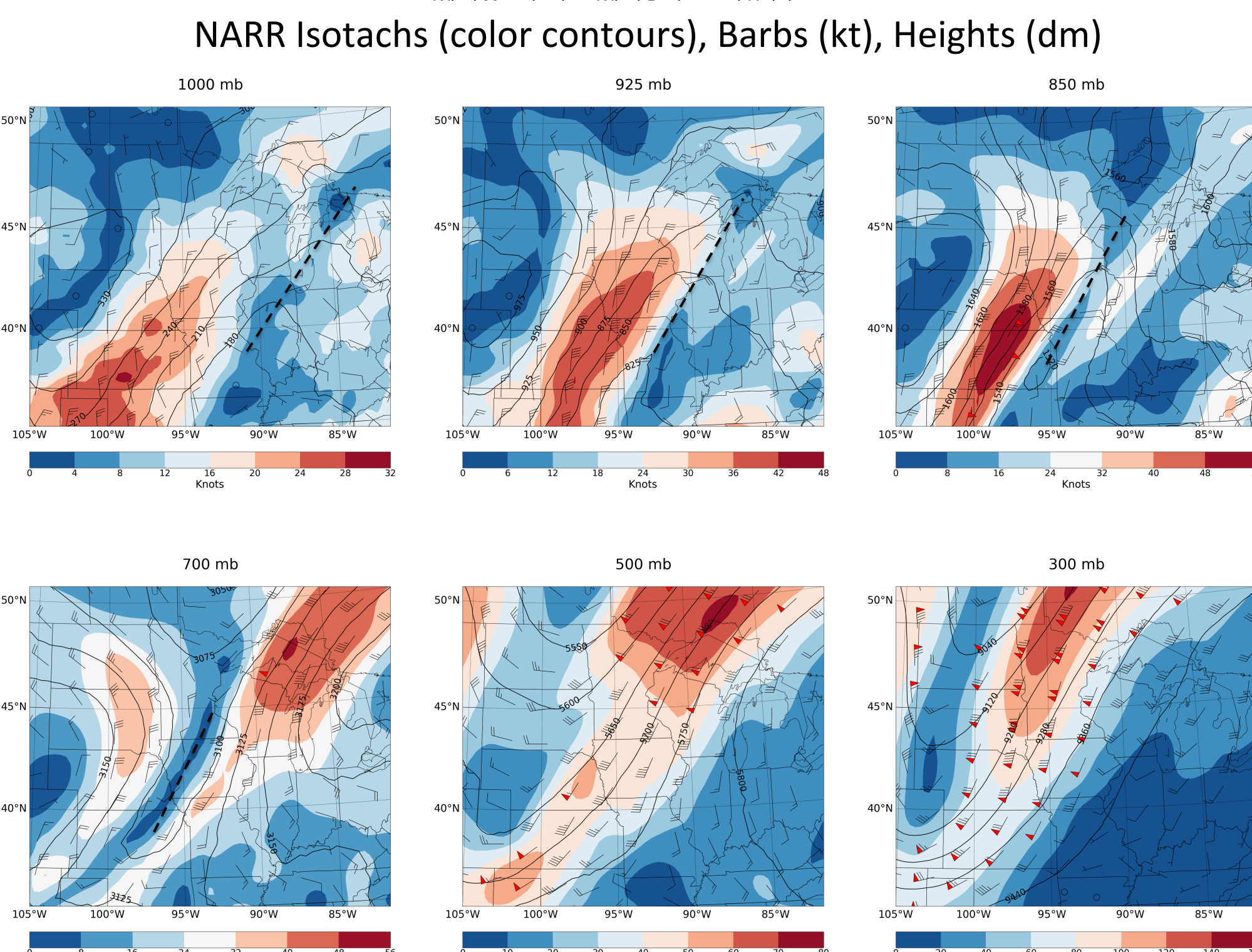
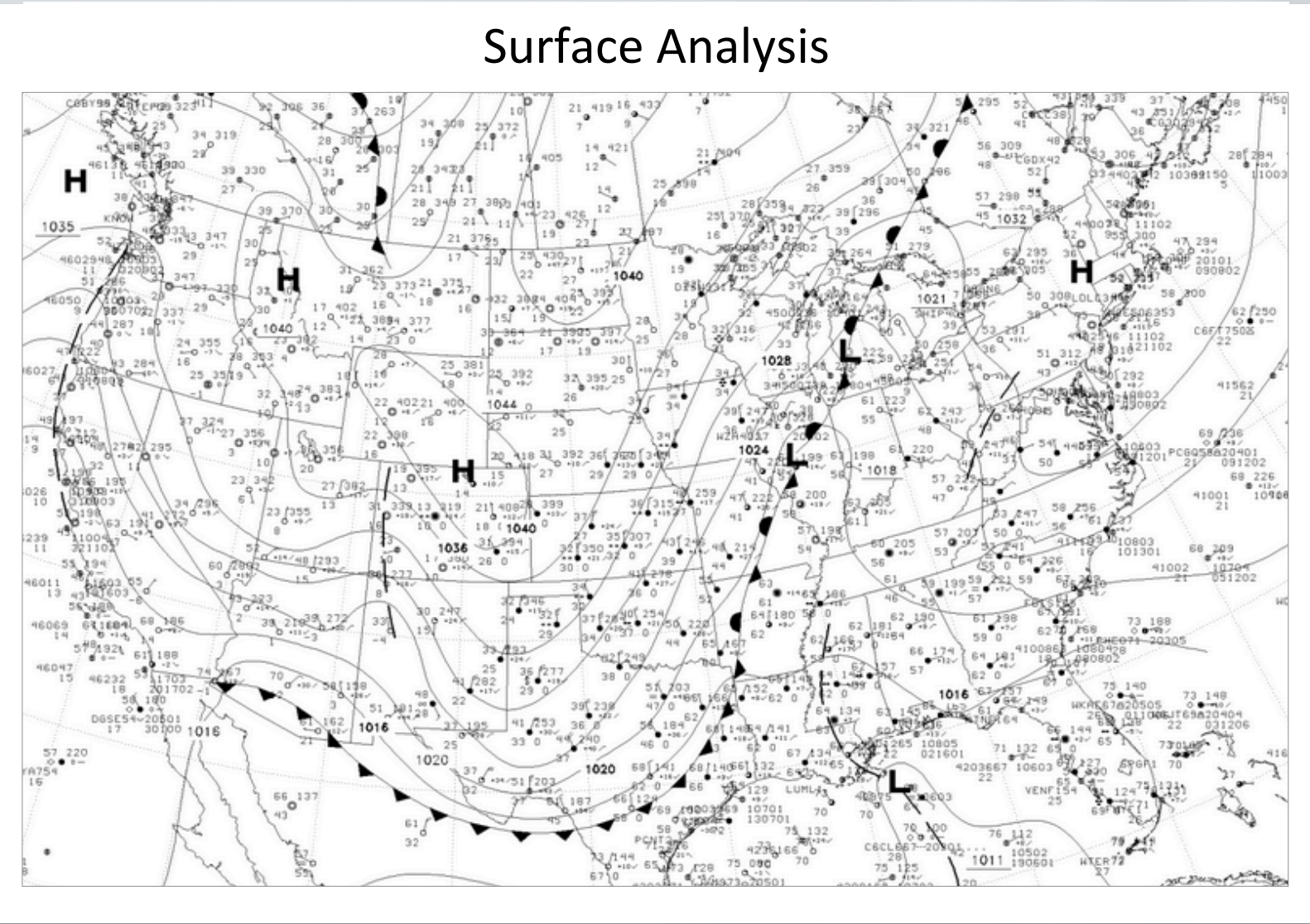
Most of the precipitation occurred in a large frontal band orientated from SSW-NNE. On May 02, volume scans from the NASA S-Band Dual-Polarimetric Radar (NPOL) observed wave formations within this frontal band, around 2 km above ground level.

Synoptic Overview (12 UTC May-02)



A positively-tilted upper-level trough was centered over the northern plains. A blocking high over the northeast prevented the trough from progressing eastward. Instead, the trough deepened and remained in place.

A quasi-stationary front provided the ascent for the band of precipitation associated with the KH-waves. The precipitation at the surface fell as rain below the KH-waves, although the rain/snow line was located just to the west across central Iowa.



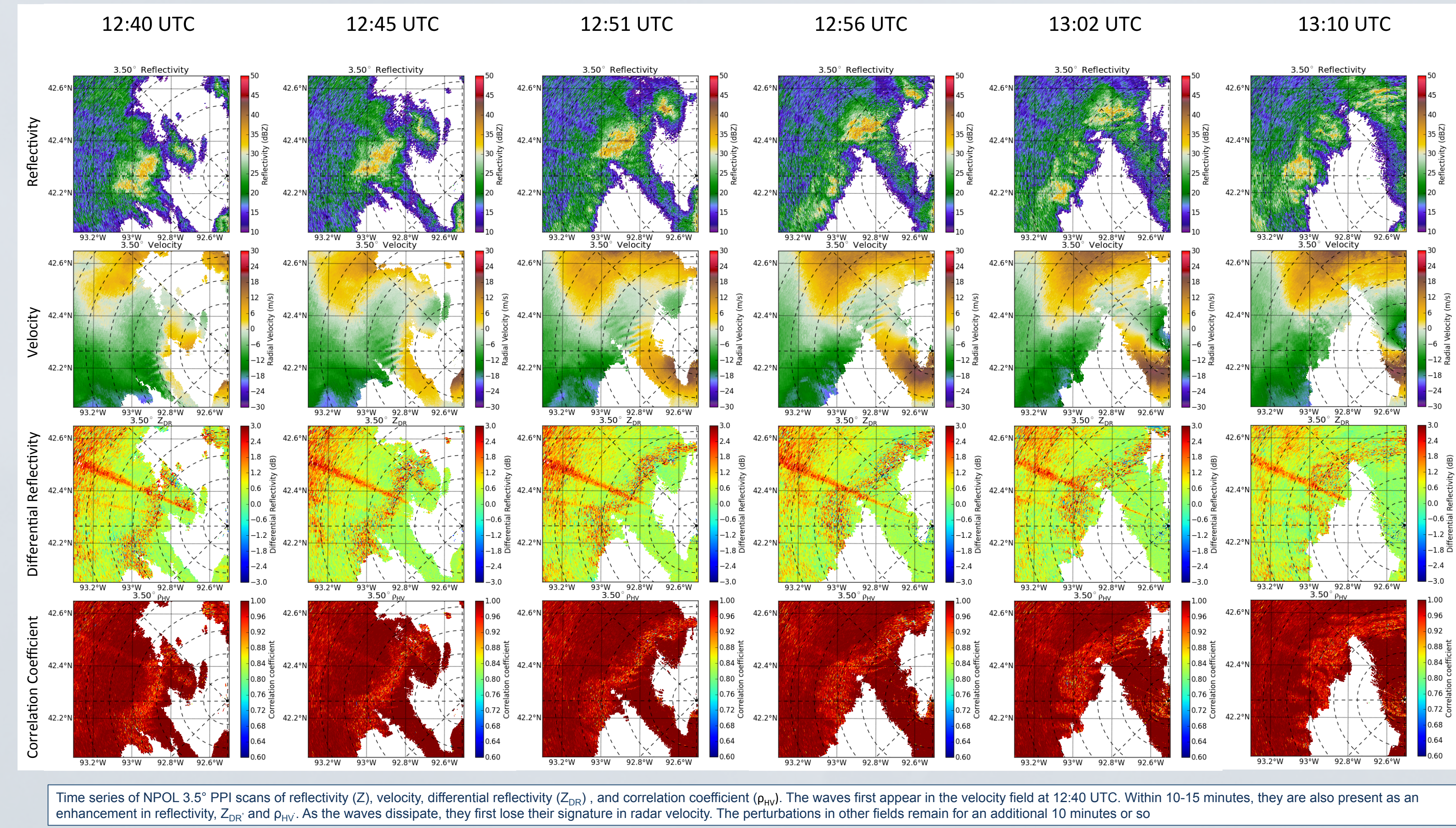
The dashed black line shows the location of the front at the indicated pressure level. The KH-waves formed within this sheared frontal zone.

At low levels, the winds reversed direction with height in association with the quasi-stationary front. The front slopes to the NW with height from near the Iowa-Illinois border at 925 mb to NW Iowa at 700 mb. Shear was enhanced by a northerly low-level jet beneath the frontal zone.

Wave Structure and Evolution

The observed waves had the following properties:

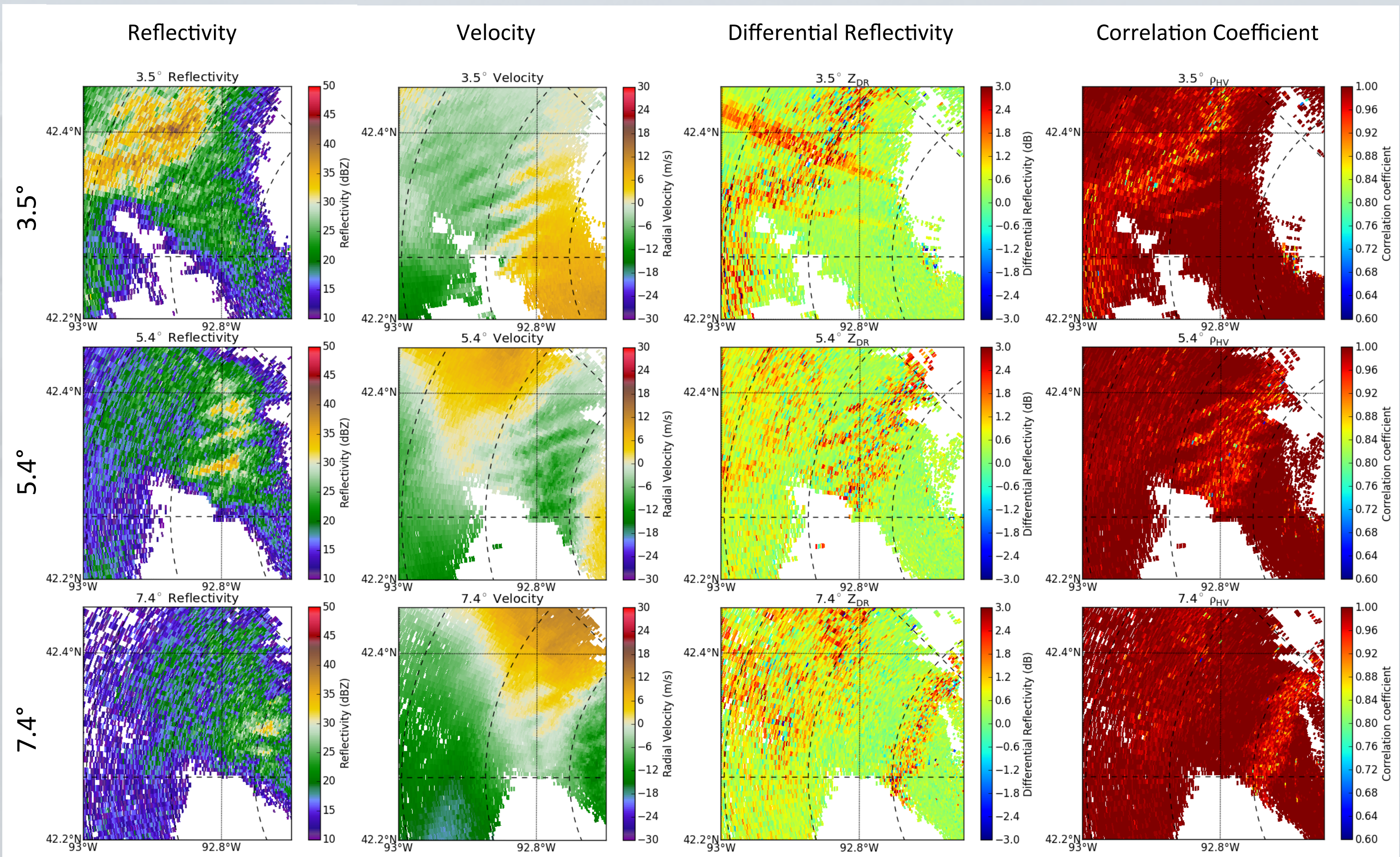
- 30 minute lifetime, 12:40 UTC – 13:10 UTC
- Propagation in the direction of the mid-level flow, SSW to NNE
- Initially only present in velocity, later in Z, Z_{DR} , and ρ_{HV} as waves grow
- Initially located 2 km AGL with a wavelength of 3 – 4 km
- Maximum vertical extent of about 2 km



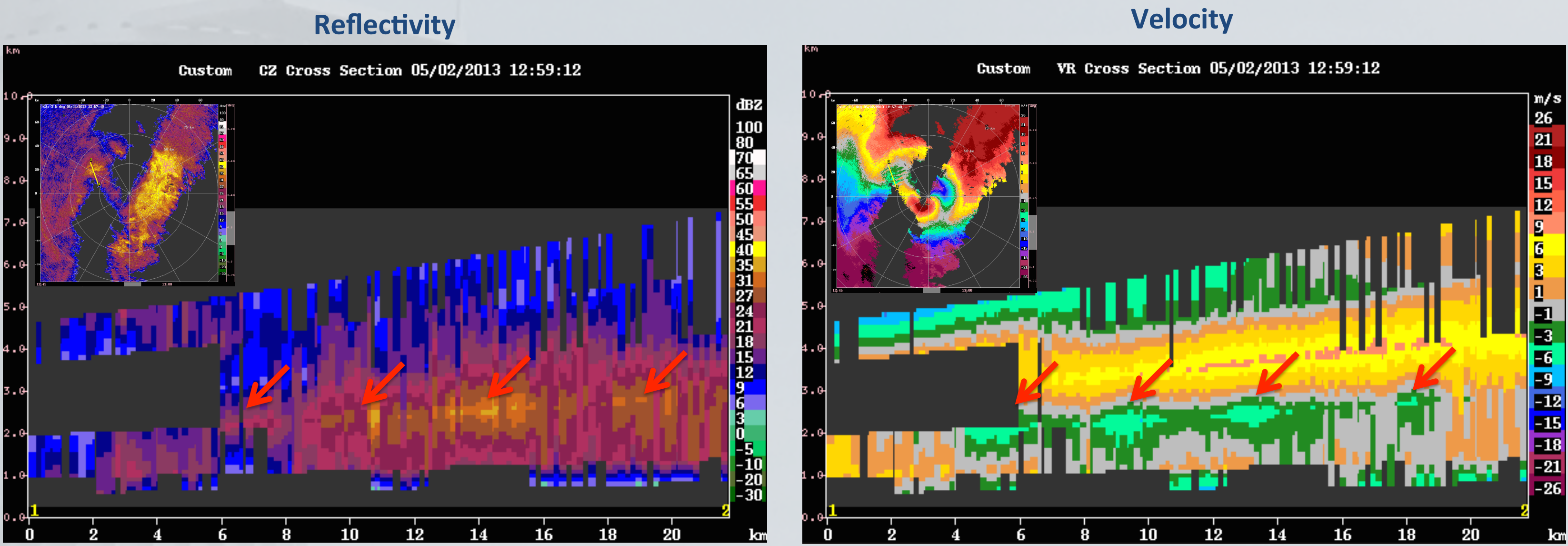
Time series of NPOL 3.5° PPI scans of reflectivity (Z), velocity, differential reflectivity (Z_{DR}), and correlation coefficient (ρ_{HV}). The waves first appear in the velocity field at 12:40 UTC. Within 10-15 minutes, they are also present as an enhancement in reflectivity, Z_{DR} , and ρ_{HV} . As the waves dissipate, they first lose their signature in radar velocity. The perturbations in other fields remain for an additional 10 minutes or so.

Vertical Structure and Microphysics

Within the wave crests, upward motion increases Z and Z_{DR} while decreasing ρ_{HV} . This combination likely results as a consequence of accretion processes including riming, condensation, and/or aggregation.

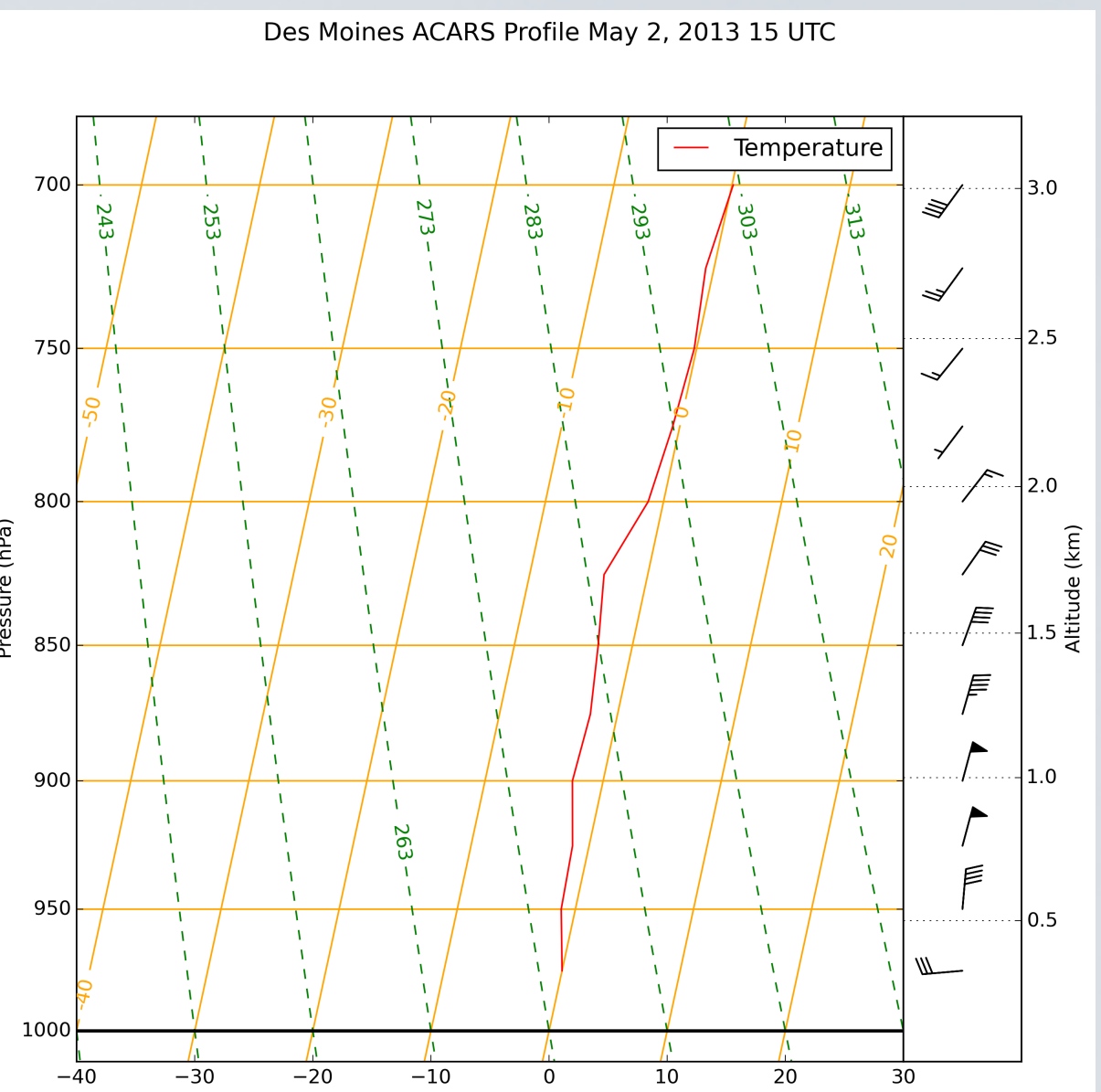
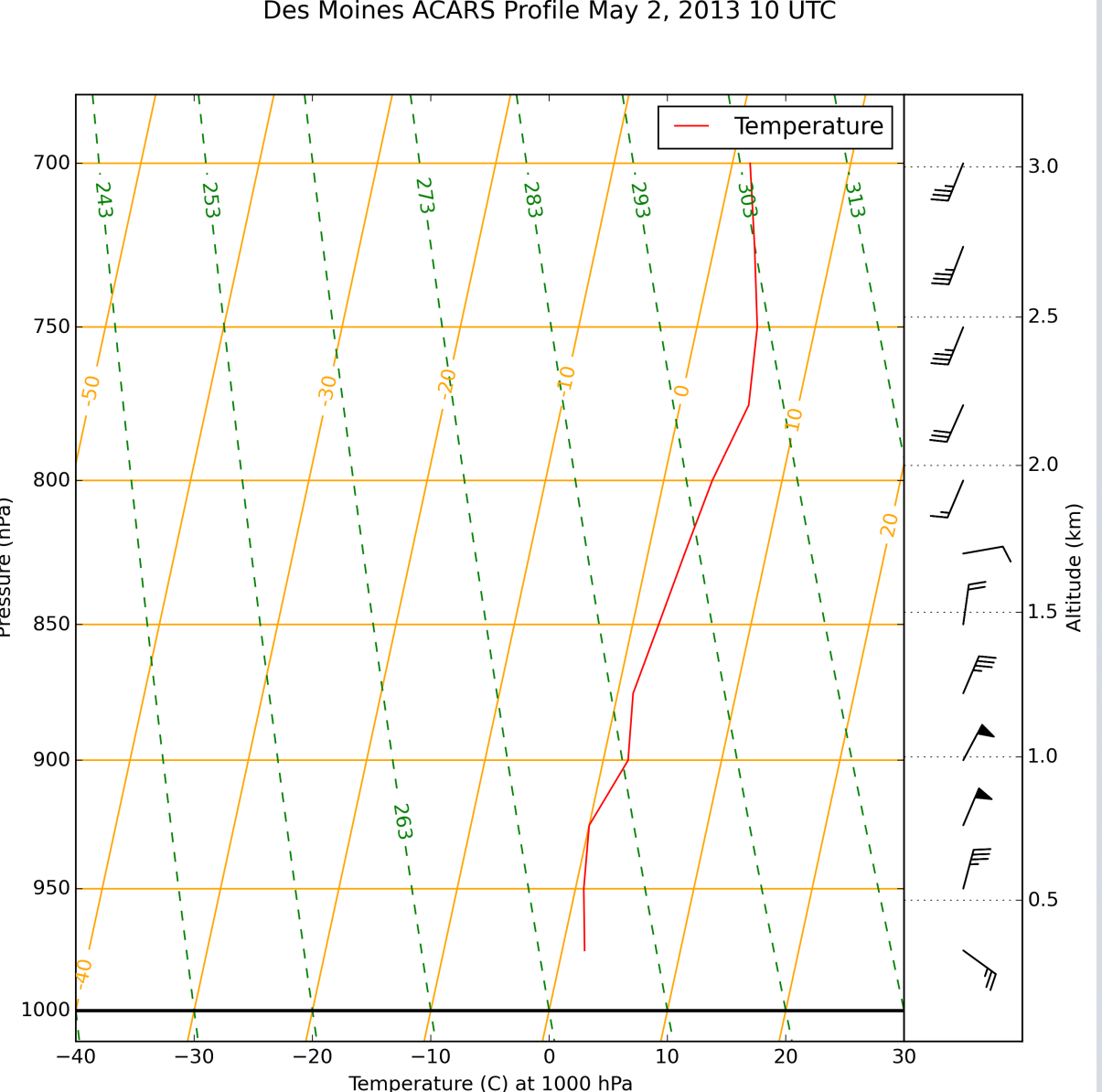


Cross sections at time of maximum vertical extent



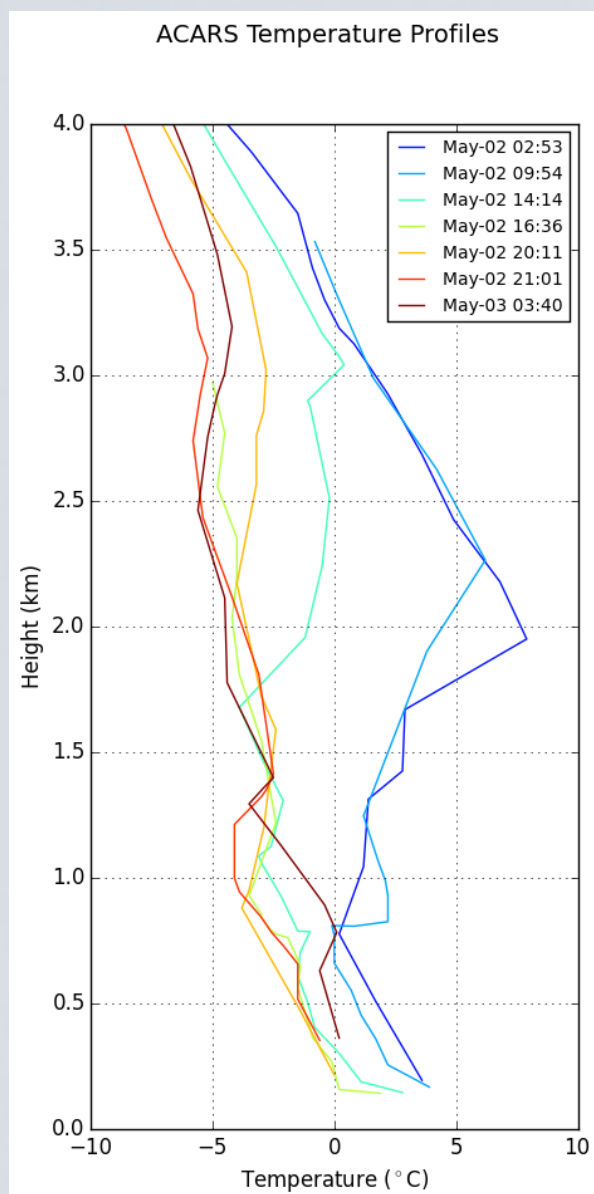
The velocity cross section (right) shows 4 distinct waves coinciding with enhancements in reflectivity (left). The wavelength is 3.25 km and the wave depth is about 2 km. Smaller-scale turbulent enhancement is also apparent in the reflectivity. Arrows denote the wave crests and associated reflectivity enhancement.

Temperature and Shear Profiles

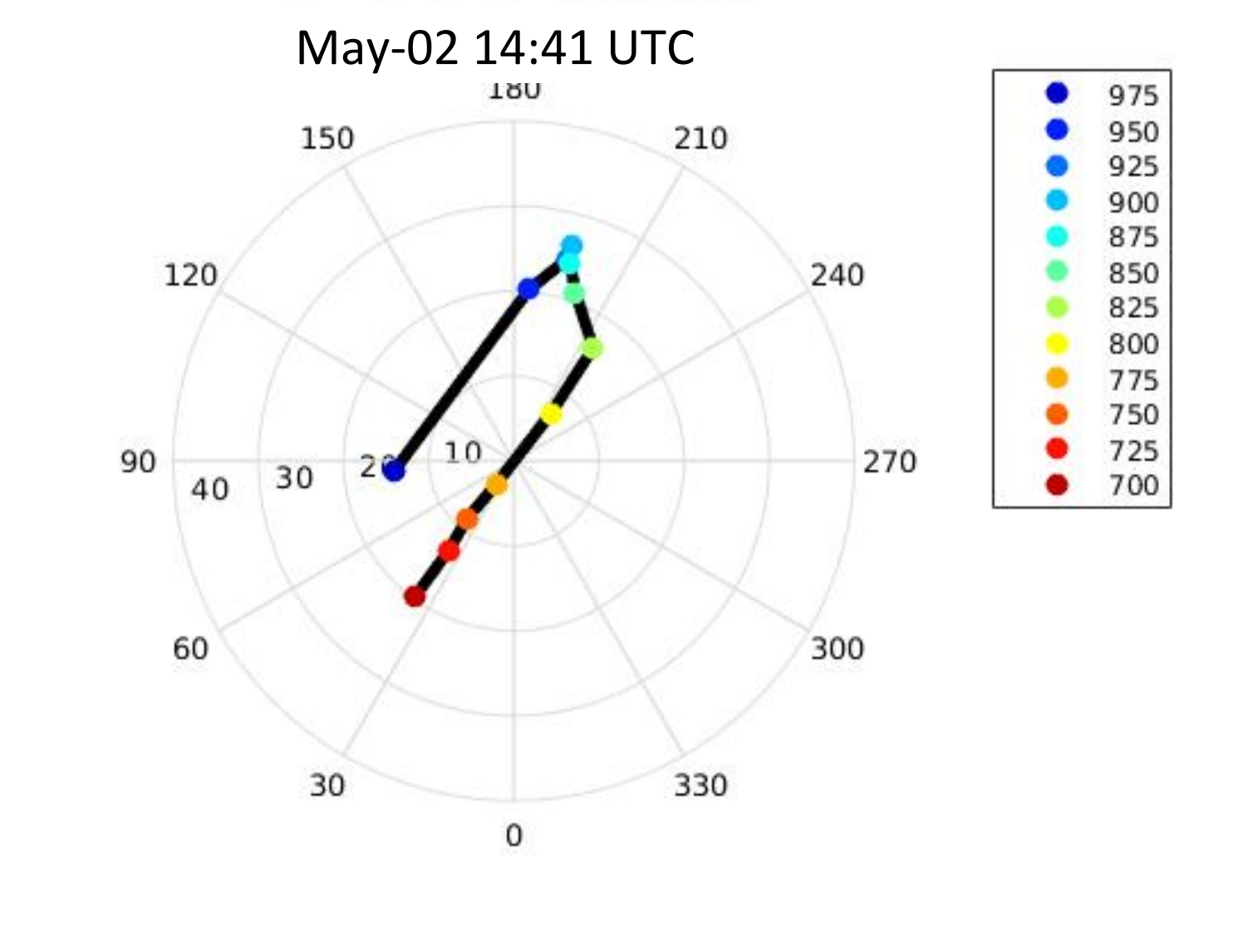
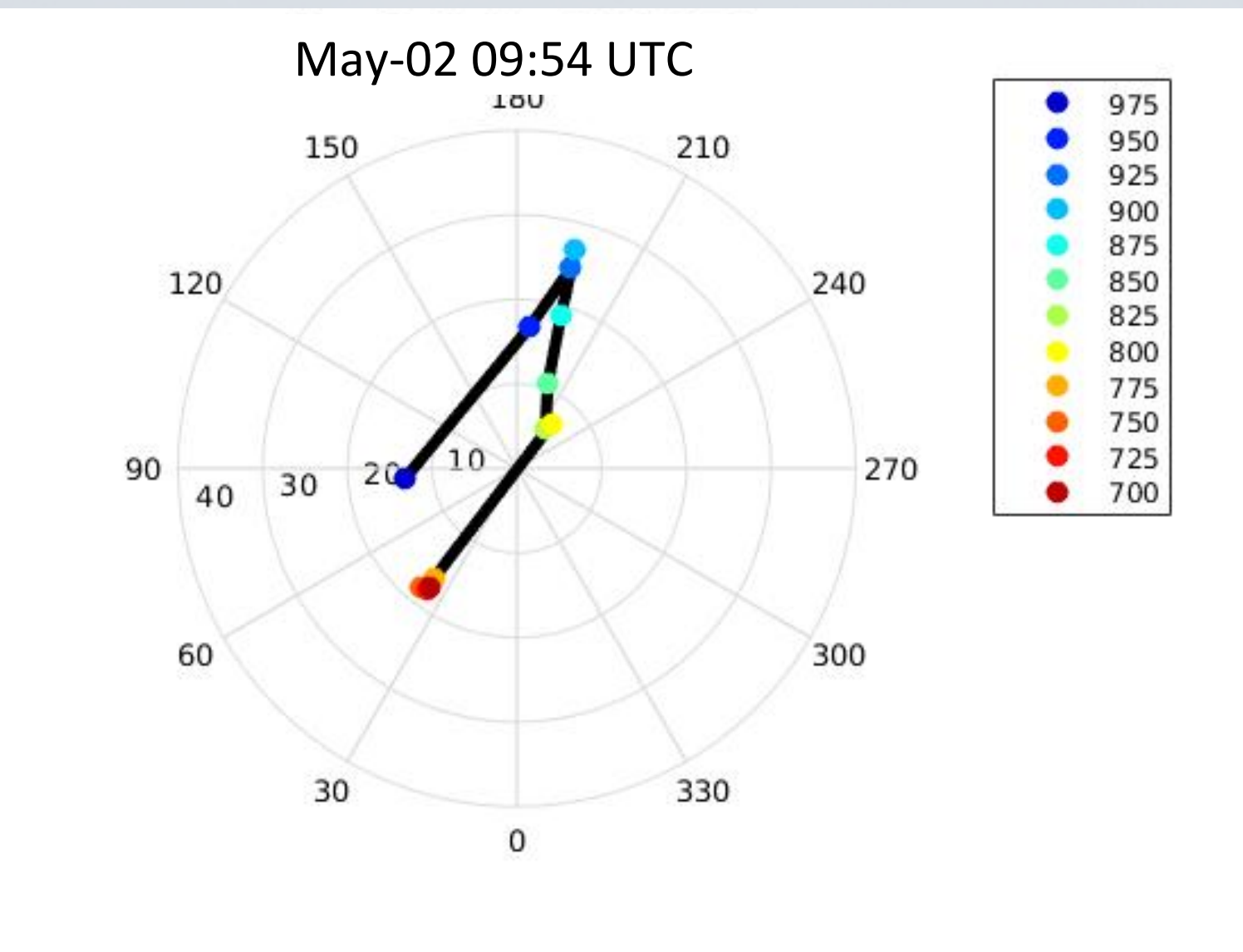


Skew-T profiles of temperature and wind from the two aircraft soundings closest to the time of the wave formation. The shear layer is higher at the time after the waves were observed (bottom panel).

The combination of a stable temperature profile and a strong sheared layer around 1.5-2 km indicates favorable conditions for the development of Kelvin-Helmholtz waves. An above-freezing layer was likely present around 2-2.5 km at the time of the waves (13 UTC), but its depth and extent can not be confirmed.



Temperature profiles derived from commercial aircraft taking off/landing from Des Moines International Airport (approximately 100 km SW of wave formation area) from 03 UTC May 2 – 03 UTC May 4.



Hodographs derived from the two ACARS profiles closest to the time of wave formation. The hodograph on the right appears to be more representative of the conditions at the time of wave formation because shear vector within the frontal zone is perpendicular to the observed waves.

The shear/frontal zone is easily distinguished in the hodographs (right). The wind reverses direction above the front.

The NPOL PPI images show that waves formed perpendicular to the shear vector within the frontal zone (925-825 mb). The Richardson number within this sheared layer is: -0.13 at 09:54 UTC and 0.20 at 14:41 UTC, both of which are below the 0.25 threshold for Kelvin-Helmholtz instability.

Conclusions

A group of Kelvin-Helmholtz waves formed and propagated within a highly sheared, stable thermal layer. Although the waves formed in the vicinity of the brightband, they further enhanced the microphysics locally within the wave crests. These turbulent enhancements are similar to those observed over mountains, (e.g. Houze and Medina 2005, Medina et al. 2007), but without the added complexities of surface topography. The enhanced microphysics often extend down to the surface in regions of higher terrain, which was not observed in this case.

The processes by which these and other features enhance precipitation microphysics is still not fully understood. Analysis could greatly benefit from *in situ* microphysical aircraft observations. Additional vertical soundings are also required to understand why the waves only form in small, localized regions. The upcoming OLYMPEx campaign offers an excellent opportunity to compare these waves to those that occur in mountainous regions.

Acknowledgements

This work was supported through NASA grants NNX13AG71G, NNX14A064G, and NNX15AL38G. Parker Malek assisted with NARR reanalysis maps. Neil Johnson and Mark Albright assisted with processing ACARS data. Stacy Brodzik assisted with radar imagery. Socorro Medina provided useful suggestions.